

Received 30 June 2023, accepted 28 July 2023, date of publication 1 August 2023, date of current version 7 August 2023.

Digital Object Identifier 10.1109/ACCESS.2023.3300951

RESEARCH ARTICLE

Testing the Validity of a Spatiotemporal Gait Model Using Inertial Measurement Units in Early Parkinson's Patients

SHUAI TAO¹, HAOYE WANG¹, LIWEN KONG¹, ZEPING LV², AND ZUMIN WANG³

¹Dalian Key Laboratory of Intelligent Medicine and Health, Dalian University, Dalian, Liaoning 116622, China

²Department of Neurology, National Rehabilitation Assistive Devices Research Center Affiliated Rehabilitation Hospital, Beijing 100176, China

³Graduate School, Dalian University, Dalian, Liaoning 116622, China

Corresponding author: Shuai Tao (taoshuai@dlu.edu.cn)

This work was supported by the interdisciplinary project of Dalian University under Grant DLUXK-2023-QN-004.

This work involved human subjects or animals in its research. Approval of all ethical and experimental procedures and protocols was granted by Sir Run Run Shaw Hospital Affiliated to Zhejiang University School of Medicine and performed in line with the Chinese GCP and relevant local laws.

ABSTRACT The subtle gait characteristics of early Parkinson's disease (EPD) patients are currently difficult to detect or require expensive, experimentally demanding testing equipment. The use of machine learning (ML) models in conjunction with inertial measurement unit (IMU) algorithms opens up new possibilities for the assessment of EPD patients. The aim of this study is to measure EPD gait using the IMU algorithm, select gait features using Recursive Feature Elimination (RFE), and classify EPD patients with healthy (HT) older adults using ML on the selected features. Firstly, 10 healthy subjects were recruited and the system parameters were validated using the double gold standard to ensure the reliability of the system. Second, 60 subjects (30 EPD patients and 30 HT elderly) were recruited to wear the system for linear walking activities and to obtain gait parameters. The results show that this system has good reliability, i.e. the best intraclass correlation coefficient (ICC) is between 0.521 and 0.941. The six best features of stride length, stance phase, stance time, swing phase variability, step speed and cadence were selected by RFE and classified by decision tree (DT) with a model accuracy of 91.6%, sensitivity and specificity of 91% and 83% respectively, and an ROC value of 0.92. Our results show that the use of the IMU algorithm with precise accuracy can detect subtle gait features and that the use of optimal gait features can well assess patients with EPD, providing a new way to detect EPD.

INDEX TERMS Early Parkinson's disease, subtle gait characteristics, machine learning, detection method.

I. INTRODUCTION

Parkinson's disease (PD) is a complex and progressive multi-system disease [1], which is caused by increased death of substantia nigra neurons in the basal ganglia of the brain. The typical manifestations of PD patients are slow movement, rigidity, and decreased self-discipline, which will bring serious motor disorders to PD patients [2]. Movement disorders may cause some special gait characteristics of PD patients, such as shorter gait length, slower gait speed, impaired

rhythm, and increased axial stiffness [3], [4]. PD is a very common disease among the elderly [5], with 1 in 1000 people over 65 years old and 1 in 100 people over 75 years old [6]. Mobility impairment is a very risky factor for PD patients, and patients with both mobility impairment and PD have a higher risk of death than those with only one of these conditions [7].

Medicine often uses the Parkinson's Unified Rating Scale [8] (UPDRS) to evaluate the degree of Parkinson's disease, but its evaluation of gait is relatively general and has certain subjective factors. Generally, a timer is used to let the patient do some walking and other actions, and the gait cannot be accurately measured. To measure the gait of PD

The associate editor coordinating the review of this manuscript and approving it for publication was Paolo Crippa¹.

patients more accurately, it is usually necessary to use expensive instruments for detection in fixed laboratories, such as photoelectric stereophotogrammetry [9], which requires the participation of special staff and cannot be used for gait monitoring in life. In recent years, portable devices have attracted wide attention from the medical industry, such as inertial measurement units (IMU) and pressure-sensitive carpets for quantifying gait [10]. This low-cost gait measurement tools have developed rapidly. Although it is relatively easy for the IMU to obtain daily gait data, it is vague how the quantitative evaluation of these gaits is compared with the one-time clinical evaluation, and whether they can replace or only enhance the current gold standard needs further verification [11].

In recent years, IMU has gradually been attached to importance by the scientific research community, and wearable IMU equipment has been used for gait detection and analysis in the laboratory or daily life [12]. For patients with early PD, gaits may change slightly, which may have serious consequences if left untreated, and a wearable IMU was now the appropriate choice to be able to detect their gait data in daily life. The wearable IMU can well-meet the requirements of not being constrained by the environment, making it possible to detect the gait anytime and anywhere [13]. According to previous reports, spatiotemporal gait parameters are of great significance in the analysis of gait detection results using wearable IMU systems [14]. However, there are few articles about the verification of wearable IMU at present. Whether it can replace expensive gait detection equipment still needs constant experimental verification.

The purpose of this paper is to propose a new IMU-based free-walking gait model. The IMU noise is analyzed by using Allen variance to observe the main sources of noise and to treat the noise to the walking cycle. The model is first processed for noise and then combined with the corresponding gait model to calculate each gait parameter.

For this purpose, we developed a daily gait device (DGE) based on the above model. The parameters that DGE can measure include step length, stride length, stride time, step frequency, step speed, support phase, swing phase, ankle joint (AJ) angle, heel strike (HS) angle, toe off (TO) angle and pressure center (COP). For the IMU part of the sole, the hardware size is small and can be embedded in the heel. It can provide relatively comprehensive real-time gait data, and the collected data can be viewed at any time through a personal computer (PC) or mobile phone application, which has good portability. For early Parkinson's patients, to intervene early, we need to obtain gait data in their daily life more. To better share data with other gold standards, validation experiments are particularly important. Using two gold standards for the first time to validate IMU spatiotemporal gait parameters can reduce data imbalance in single gold standard validation of single parameters, making IMU data more medical reference value and making daily data more available. Recruited elderly patients with early PD and healthy elderly people carried out the straight-line walking experiment and collected

corresponding gait data, and calculated the mean value and coefficient of variation of gait parameters of the PD group and healthy group respectively. Previous experimental studies have found that PD patients may also have slow gait or abnormal gait posture adjustment in the early stage or before they have no gait disorder [15], [16]. Through this experiment, it was also found that the variation coefficient of TO angle, HS angle and stride time of EPD patients also changed significantly, which provided a necessary argument for EPD patients to have insufficient ankles flexion.

II. RELATED WORK

Wearable technology is now more prevalent in the medical industry, and its rapid development can gradually shift from the original testing in the laboratory or fixed places to non-fixed places. For the calculation of spatiotemporal gait parameters, accurate estimation of step size is an important parameter. Next, we summarized the most advanced step size estimation techniques that are currently closest to our work.

Wu et al. used 2 MPU-9150 sensors mounted at the left and right ankles, respectively, with an inverted pendulum model [17]. They calculated the distance of a single step by multiplying the leg length by the sine of the change in leg direction at each step. Their calculation of error was based on the total walking distance, and the error of a single step was not analyzed. Pepa et al. used the accelerometer that came with the smartphone and developed a corresponding program to collect data on movement gait [18]. They use an inverted pendulum model to estimate step size and validate it with other devices. Wang et al. presented a biomechanical model of knee flexion, and they used four MPU-6050 sensors mounted to the left and right thighs and calf, respectively [19]. They used a double pendulum model to estimate step size, taking into account the asymmetry of step size and gait, but they ignored the displacement of the hip joint in the direction of motion, resulting in a bias in step size estimation. The accuracy for single pendulum model or double swing model methods usually depends on the parameters set in advance or estimated for calibration, which also causes uncertainty in the accuracy.

Recently Anderson et al. using 4 MPU-6050 and 4 Ultra Wideband (UWB), solved the limitations of the above study, but they used 8 sensors, the data processing of 8 sensors increased the difficulty and complexity of the system, and the stability of the system for outdoor needs further demonstration [20]. The current application of machine learning methods allows for more sub-stages, but using sensor algorithms has lowered computational complexity and more timely response times. So, in daily wear detection sensor algorithms are still preferred. For using a single IMU, it is difficult to take into account the asymmetry of the gait space. Therefore, we use 4 IMUs worn on the bottom of the foot and ankle and use low-power components. No need to set parameters in advance for precise estimation. And it is a low-cost device with functions such as user feedback.

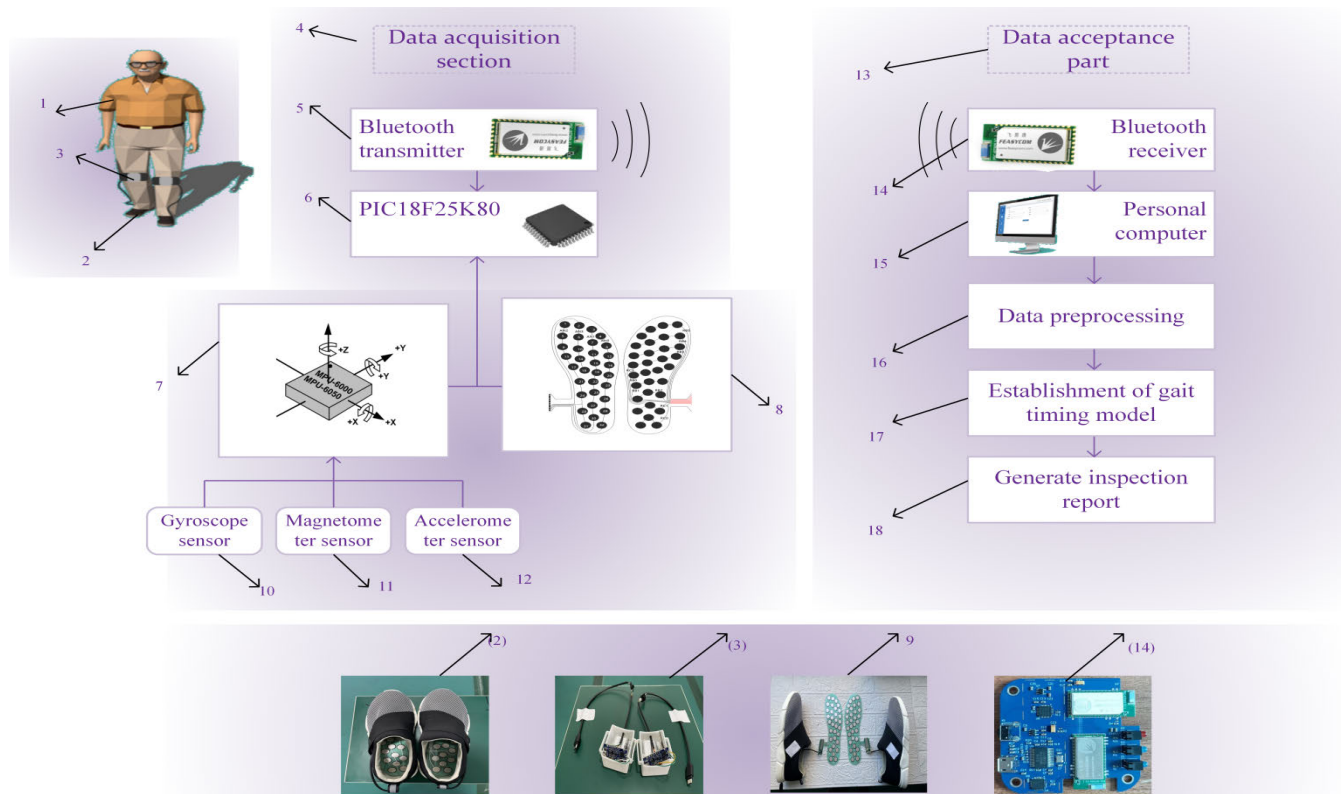


FIGURE 1. Experimental supporting facilities: 1; Testers, 2; Sampling shoes ((2) is the internal drawing of sampling shoes), 3; Lower leg sampling module ((3) for appearance), 4; Data acquisition part, 5; Bluetooth transmitter, 6; MCU, 7; Inertial measurement unit, 8; Full pressure film pressure sensor, 9; circuit board for the foot pressure data acquisition device, 10; Gyroscope sensor, 11; Magnetometer sensor, 12; Accelerometer sensor, 13; Data acceptance part, 14; Bluetooth receiver ((14) is a Bluetooth receiver integrated circuit), 15; Personal computer, 16; Data preprocessing, 17; temporal gait model building, 18; Generate inspection report. The blue line represents the data flow.

III. MATERIALS

A. CIRCUIT DESIGN

1) CIRCUIT OVERVIEW

The original intention of the development is for medical wear, and the scientific nature of the design and the stability of the circuit is fully considered in the circuit design. As shown 8 in Fig. 1, for the foot pressure membrane pressure sensor whose size is based on different shoe sizes, 32-foot pressure points are set for each of the left and right feet, enabling detailed delineation of the foot area. As shown 9 in Fig. 1, the board is a foot pressure data acquisition device, a board size of 55 mm × 25 mm, in the production of the need to use resin adhesive encapsulation to enhance the board’s ability to resist pressure. As shown in (2) in Fig. 1, the finished product with the foot pressure sampling shoes was installed. As shown in (3) in Fig. 1, for the lower leg data acquisition equipment, the board size is 43 mm × 18 mm. As shown in (14) in Fig. 1, for the left and right leg data receiving equipment, the plate size is 56 mm × 56 mm. For this system, the main electronic components are IMU, low power Bluetooth, micro control unit (MCU, PIC18F25K80) produced by Microchip Technology, USA, etc.

TABLE 1. Foot pressure membrane sensor parameters.

Parameters	Numerical Value	Unit
Measurement range	0-100	kg
Sensing point diameter	13-15	mm
Sensor thickness	≤0.25	mm
Hysteresis	<10	%
Drifting	<10	%
Precision	±10	%

2) FOOT PRESSURE FILM PRESSURE SENSOR

Foot pressure film pressure sensor uses a flexible foot pressure sensor with array distribution, which is made by a precision printing process, transferring nano force-sensitive materials, silver paste and other materials to the flexible film substrate and curing by drying. The basic parameters are shown in Table 1.

3) IMU

As shown 7 in Fig. 1, the 9-axis motion sensor is used, which is composed of a 3-axis gyroscope, 3-axis accelerometer

and 3-axis magnetometer, and the IMU is used to measure the motion information of the measured object [21]. The system uses a power supply voltage of 3.3 V, an accelerometer range of ± 16 g, a gyroscope range of $\pm 2000^\circ/\text{sec}$, and Inter-Integrated Circuit (I2C) communication, etc. Sampling in three directions of the x-axis, z-axis and y-axis can flexibly and accurately collect data from all directions for analyzing spatiotemporal gait parameters.

4) DATA COMMUNICATION

As shown in 5 and 14 in Fig. 1, at present, the medical system mostly uses Bluetooth communication, which has a wide range of applications on the Internet of Things. Most platforms support Bluetooth communication, so using this communication can improve the application range of medical devices on the Internet of Things. The communication module adopts the FSC-BT909 Bluetooth module from Feasycom, Shenzhen, China, which is a dual module with Bluetooth 4.2 audio and data Bluetooth, and supports both BR/EDR and LE, transmitting power +18.5 dBm, voltage range 2.3-3.6 V, working frequency band 2.402-2.480 GHz, size 13 mm \times 26.9 mm \times 2.4 mm, capable of high-speed transmission. With the integrated antenna, the communication range is up to 500 m and has a strong anti-interference capability, which fully meets the system's usage range and can avoid data instability when the communication threshold is reached. The data is sent and received in strict accordance with the set protocol, and the sensor data is sent with a time stamp.

IV. METHODS

A. TIME-SEQUENCE GAIT MODEL BASED ON IMU

1) PLANTAR PRESSURE ANALYSIS

When the sensor is subjected to pressure, the resistance decreases with the increase in pressure, and its piezoresistive characteristics show a power function relationship between resistance and pressure, and the inverse of the resistance is nearly linear with the pressure, each sensing unit can be regarded as an independent variable resistance, through the hardware and software to process the data conversion can measure the corresponding force value.

The pressure distribution in the foot varies during movement ((c) in Fig. 2), and it is important and inevitable to divide the pressure into the foot into different areas for identification. The COP can be calculated from the foot pressure sampling pointed and presented in images (Fig. 2 (a) and (b)) as the central distribution of COP, which facilitates the gait assessment of the test person by the medical personnel afterward. The COP distribution can be used to analyze the fall detection problem and prevent it in advance, which is an important indicator for judging walking stability and balance problems, and the closer the COP distribution is to a linear trend, the better the stability of the tested walking process.

For the walking process, in addition to paying close attention to the COP changes at the same time the average pressure

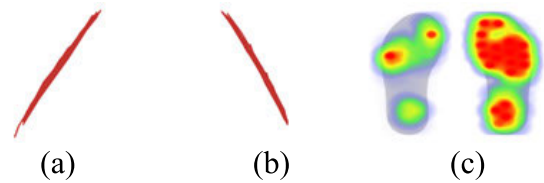


FIGURE 2. Free walking cop distribution. (a) ; Left foot cop distribution in free walking. (b); Right foot cop distribution in free walking. (c); Visualization of foot pressure during walking.

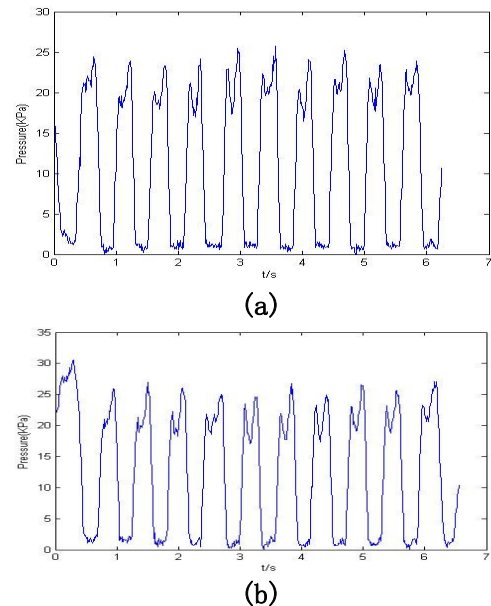


FIGURE 3. (a) and (b) are the average pressure distribution curves of the foot pressure when the left and right feet walk freely, respectively.

curve still has a very significant gait relationship, which can be used for the problem of freeze gait (FOG) recognition [4] when the accelerometer has difficulty capturing the untraveled or no effective step. In the stepping process and in the static state, the force on the foot pressure film pressure sensor is the vertical component of gravity on the foot pressure film, and the pressure F is almost equal to the component of gravity G , so the average pressure distribution curve can be obtained (Fig. 3). The maximum value of the curve peak are when one side of the foot is completely on the ground, and the other side is in the air.

2) IMU ACQUISITION UNIT

The tester needs to wear the right shoe size when recording the gait in life, and the data is sent to the PC (15 in Fig. 1) receiver via Bluetooth of the collection device for data interaction. Since the IMU tri-axis accelerometer data are susceptible to interference, the calculation of the relevant gait data is susceptible to serious effects of interference components, and here the acceleration data are filtered using arithmetic average filtering (16 in Fig. 1) to improve the accuracy and stability of the calculated data. The quaternion can be solved from the original data for attitude saving, and

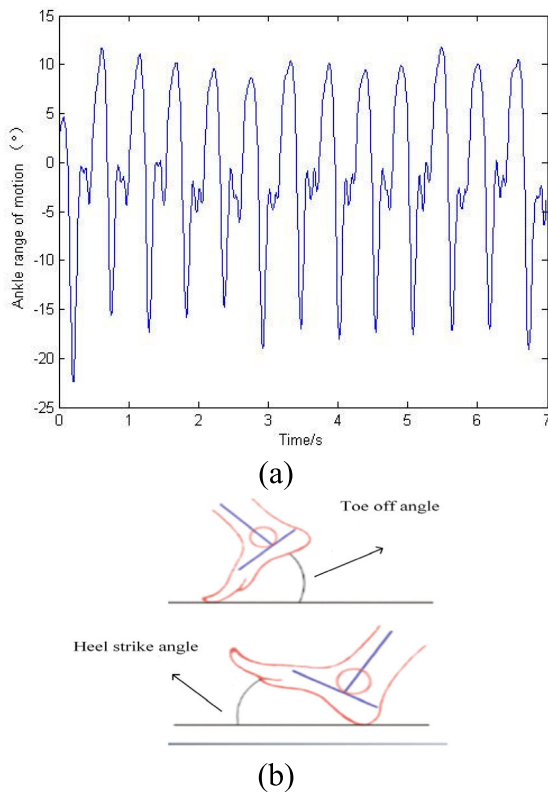


FIGURE 4. (a) ; Ankle joint mobility. (b); Heel strike angle, toe off angle.

the corresponding attitude angle can be solved by quaternion [22]. To reduce the integration error of the angular velocity meter for a long time, the complementary filtering method is used to fuse the data of the accelerometer and angular velocity meter [23].

As the IMU can be affected by a variety of noises, it can affect the final calculation results. We used the Allen algorithm to analyse the IMU noise and found that zero bias instability was the main source of noise [24]. As the gait parameters are in a cyclic state during walking, we propose a cycle-setting approach to eliminate zero bias instabilities, whereby the left and right feet reach a cycle of relative resting points, so that the corresponding axis is set to zero to eliminate zero bias noises.

For the angle problem in the motion state, the heel landing (HS) angle, toe off the ground (TO) angle ((b) in Fig.4) and ankle joint activity (relative to the joint activity in the initial position of standing [25], (a) in Fig. 4) were measured respectively. For spatiotemporal gait parameters, step length, step speed, step time, cadence, swing phase and stance phase are calculated respectively.

3) STEP LENGTH

The distance between the heel of one foot touching the ground and the heel of the other foot touching the ground. The axial acceleration of the accelerometer sensor in the travel direction (X-axis) can be used to calculate the travel step length, and

the corresponding step length can be calculated by double integration of the X-axis acceleration data. The calculation formula is as follows.

$$d = \iint (a_x(t) - a_{avg}(t))dt \quad (1)$$

where d denotes the step size, a_x denotes the x-axis acceleration of the triaxial accelerometer, and a_{avg} denotes the average of all accelerations in a single step. Since the sensor contains a DC component in the acceleration output, to eliminate this DC component, this a_{avg} needs to be subtracted before calculating the dual integration.

In the walking process, the walking direction is the X-axis direction of the IMU, and the acceleration is mainly generated by the swing of the wearer's body during the walking process, as well as the acceleration generated by the interaction between the foot and the ground when landing and lifting [26]. The latter collision with the ground can be seen as an elastic collision, when the walking speed is from slow to fast, the size of the elastic force will not directly affect the maximum acceleration and minimum acceleration but will make the average value of acceleration becomes larger [27]. To remove the effect of this elasticity, the following correction factors are used [28].

$$d_h = k \times \frac{a_{x(avg)} - a_{x(min)}}{a_{x(max)} - a_{x(min)}} \quad (2)$$

d_h is the step correction factor; k is a constant; $a_{x(avg)}$ is the average value of single-step acceleration; $a_{x(min)}$ is the minimum value of a single-step x-axis; $a_{x(max)}$ is the minimum value of the single-step x-axis. Therefore, the actual step (D) can be calculated according to the following formula (3).

$$D = d \times d_h \quad (3)$$

4) STEP SPEED

Walking distance per unit time, unit: m/s. It is calculated as (4)-(5).

$$v = \frac{D}{t_D} \quad (4)$$

$$D = \sum_{i=1}^n d_i \quad (5)$$

where D is the total distance traveled and t_D is the time to travel the total distance. The total walking distance D is calculated by summing the step lengths calculated by equation (1), where n is the number of steps taken by the tester.

5) CADENCE

The number of steps walked per unit of time (steps/min). The cadence can be calculated from Fig. 3. The periodic shift of foot pressure corresponds to the periodic shift of gait, and a cycle includes peaks and valleys. The calculation formula is as (6).

$$f_c = \frac{n}{T} \times 60 \quad (6)$$

where f_c is the step frequency, n is the number of test steps, T and is the n step duration in seconds, then you can calculate the number of steps in 60 seconds that is the cadence.

6) CALCULATION OF SWING PHASE AND STANCE PHASE

In a single stride, the support phase time is the HS to TO time, and the swing phase time is the time from TO to HS of a particular side foot. Therefore the stance phase and swing phase can be calculated by using equations (7)-(8).

$$T_{SW} = \frac{t_{HS} - t_{TO}}{t_s} \times 100\% \quad (7)$$

$$T_{ST} = \frac{t'_{TO} - t_{HS}}{t_s} \times 100\% \quad (8)$$

where T_{SW} and T_{ST} are the swing phase and support phase, respectively, t_s is the single stride time, t_{HS} is the single stride HS moment, t_{TO} is the single stride TO moment, and t'_{TO} is the next stride TO moment.

B. PARTICIPANTS

We divided the participants into two groups i.e. group A and group B.

Group A: 10 participants (5 male and 5 female) were recruited from the community and were healthy participants without abnormal gaits, with an average age of 25 years, a height distribution range of 158 cm-180 cm and a weight distribution range of 48 kg-70 kg.

Group B: Thirty patients with EPD were recruited from patients with Parkinson's disease at Run Run Shaw Hospital, Zhejiang University School of Medicine (Hangzhou, China), and 30 HT volunteers of relatively similar age, height, weight and shoe size (without orthopedic or neurological disease) were recruited as the experimental reference group. Information about this group is shown in Table 2. Where PD patients underwent the Mini-mental State Examination (MMSE) results were greater than 26 [29], excluding the effect of cognitive dysfunction and dementia on the results, where the level of education: was 6-12 years. For the Hoehn-Yahr (H&Y) classification [30], all patients with stages 1-4 can walk on their own, and stage 5 patients are physically restricted to a wheelchair or bed with difficulty walking independently. Usually, stage 1-2 is classified as EPD patients and treated mainly with medication. In this trial, all PD participants were \leq stage 2 (stage 1: $n=1$; stage 2: $n=4$), i.e., participants were diagnosed as early-stage patients. None of the participants experienced gait freezing during the experiment.

All gait experimental procedures were conducted by movement disorder specialists according to standardized consensus criteria. Participants were informed of the purpose of their participation and signed a written consent form, their participation in this gait assessment was voluntary and could be terminated at any time their participation and consent was obtained for the use of the data. This study was approved by the Ethics Committee of the Sir Run Run Shaw Hospital Affiliated to Zhejiang University School of Medicine.

TABLE 2. Information on healthy participants and early PD patients in group B.

	HC(n=30)	PD(n=30)
Age	65.60±10.51	66.40±8.39
Gender (m: f)	20:10	20:10
Height (cm)	167.2±5.11	163.2±6.26
Weight (Kg)	65.5±6.23	62.1±9.61
Shoe Size (CHN)	40.6±2.19	40.0±2.00
MDS-UPDRS III		23.80±4.09
H-Y	\	1.80±0.45
MMSE		28.80±0.84

C. EXPERIMENTAL DESIGN

The wearable parts of the system consist of sampling shoes and a calf collector. The sampling shoes consist of an IMU, a foot pressure sensor and a power supply, and the calf collector consists of an IMU and a Bluetooth transmitter.

Zebris®-FDM system, consisting of 22,528 sensors, dimensions: 307.0 × 60.5 × 2.5 cm, measuring range: 1-120 N/cm², using three groups forming a foot pressure analysis trail of approximately 9 m [31].

The Vicon®-512 system [32], consisting of six infrared-sensing cameras and reflective markers, acquires motion trajectories by tracking the reflective markers [33].

Group A: Subjects are required to choose the appropriate shoe size for the sampling shoes and tie the calf part behind the calf with an elastic band. This device will not change the walking habits of the wearer, so no gait abnormalities will occur due to walking discomfort. Reflective markers on the toe and heel for the camera to obtain motion tracking. All equipment was turned on. Subjects were required to walk at normal speed on the analysis trail, as in Fig. 5. Each tester walked 6 complete gait cycles.

Group B: EPD patients wore only this system DGE device and performed linear walking in the laboratory to collect and record data for subsequent analysis. Each tester walked 6 complete gait cycles.

D. FEATURE SELECTION AND CLASSIFICATION MODEL

The temporal gait features collected from DGE and the coefficients of variation (stride length variability, stride time variability, swing phase variability, and stance phase variability) were used to construct the DT classifier by a total of 14 features.

RFE is a wrapper-based feature exclusion algorithm that searches for the best subset of features in the space by executing an optimization algorithm [34]. The importance scores of each feature are calculated by feeding a set of 14 features as an initial feature subset into the DT classifier. Then, the lowest importance score is eliminated from the current subset of gait features to obtain the remaining subset of gaits. Then, the above steps are repeated for filtering until the desired



FIGURE 5. Experimental system setup.

number of features is reached. This method automatically eliminates feature subset redundancy to produce better and more compact gait feature factors.

E. DT CLASSIFICATION ALGORITHM AND APPLICABILITY

The DT algorithm is a data mining induction technique that uses either depth-first greedy or width-first methods to recursively partition a recorded data set until all data items belong to a specific class. The DT consists of three parts: a root node, an internal node and a leaf node, which is a flowchart-like tree structure where each internal node represents a test condition on an attribute, each branch represents the result of the test condition and each leaf node is assigned a class label [35]. The DT classification technique is divided into two stages, tree construction and tree pruning, with tree construction proceeding from the top downwards. At this stage, the tree is recursively partitioned until all the data items belong to the same class label. Compared to other algorithms, DT is simple and fast, suitable for small data samples, and can handle noisy data with high accuracy [36]. The DT classification algorithm was chosen as we had a small training set of samples and needed high accuracy and speed.

F. STATISTICAL ANALYSIS

All statistical analyses for this data analysis were performed using spss version 23. All gait data were tested by the Kolmogorov-Smirnov test and screened for normality.

The intraclass correlation coefficient (ICC) was used to compare the confidence levels between different test systems using the Two-way random versus absolute agreement model, where the confidence interval was set to 95%. ICC can analyze problems between data. Among them, $ICC < 0.5$ has poor reliability, $0.5 \leq ICC \leq 0.75$ has general reliability, $0.75 < ICC \leq 0.9$ has good reliability, and $ICC > 0.9$ has excellent reliability.

Bland-Altman plots were used to evaluate the intra- and inter-assessor reliability and to compare the consistency between DGE and Zebris® and Vicon®. The horizontal x-axis is the average of the data measured by the two systems, and the vertical y-axis is the difference between the two systems. The upper and lower red dashed lines indicate the upper and lower limits of the 95% agreement limits, i.e., 1.96 times the standard deviation; the yellow horizontal dashed line is where the mean value of the difference is 0, and the middle blue solid line indicates the mean value of the difference.

The independent samples t-test was used to compare the mean difference between the two systems and a p-value set at 0.05 was considered statistically significant.

V. RESULTS

A. GROUP A: CONSISTENCY OF GAIT PARAMETERS

The ten HT subjects walked 6 steps freely and calculated the mean of each of the left and right foot gait data, i.e., 20 samples each of step length, stride time, stance time, swing time, stance phase, swing phase, HS and TO (including left and right foot), and 10 samples each of step speed and cadence. The Zebris® (ZE) and Vicon® (VI) data were used as gold standards to plot Bland-Altman plots (Fig. 6) using the gait data measured by DGE, respectively.

The differences in step length, stride time and step speed in the Bland-Altman plot for ZE-DGE are within the upper and lower limits of consistency and have an excellent agreement; most of the differences of cadence, stance phase and swing phase are within the upper and lower limits of consistency and have good agreement. For the Bland-Altman plot of VI-DGE, the difference in step lengths in are in the upper and lower limits of consistency, with excellent consistency; the difference in stride time, step frequency, and step speed are mostly in the upper and lower lines of consistency, with good consistency.

B. GROUP A: CORRELATION OF GAIT PARAMETERS

DGE was compared with ZE and VI for the correlation, respectively, and ICC and significance (p) analyses were performed for the temporal gait parameters step length, stride time, stance time, swing time, HS, TO, step frequency, step speed, support and swing phases, respectively, and the results were recorded in Table 3, where the support and swing phases were compared with ZE only. Where p ranges from 0.000 to 0.322 with good overall significance and ICC ranges from 0.572 to 0.941 with good overall correlation.

The following results can be seen through the ICC results analyzed for 10 subjects in the same experimental situation. The results of the DGE and ZE left foot data are as follows: step length results ($ICC=0.922$, $p = 0.001$) have excellent reliability, stride time results ($ICC=0.936$, $p = 0.000$) have excellent reliability, stance time results ($ICC=0.936$, $p = 0.000$) have excellent reliability, swing time results ($ICC=0.655$, $p = 0.102$) have general reliability, stance phase results ($ICC=0.574$, $p = 0.110$) have general reliability, and swing phase results ($ICC=0.572$, $p = 0.111$) have general reliability. The results of the right foot data are as follows: step length results ($ICC=0.835$, $p = 0.005$) have good reliability, stride time results ($ICC=0.933$, $p = 0.000$) have excellent reliability, stance time results ($ICC=0.711$, $p = 0.026$) have general reliability, swing time results ($ICC=0.783$, $p = 0.034$) have good reliability, stance phase results ($ICC=0.724$, $p = 0.034$) have general reliability, and swing phase results ($ICC=0.720$, $p = 0.036$) have general reliability. As shown in Table 3.

TABLE 3. DGE and Zebris®, Vicon® Intra-class correlation coefficient (ICC) and significance value of data statistics.

		Position (foot)	Equipment	mean and SD	System group (ICC)	ICC	Sig (p)	Reliability	
Step length (m)	L		DGE	0.676±0.026			\		
			Zebris®	0.677±0.033	DGE: ZE	0.922	0.001	Excellent	
			Vicon®	0.685±0.041	DGE: VI	0.802	0.012	Good	
	R		DGE	0.672±0.036				\	
			Zebris®	0.687±0.053	DGE: ZE	0.835	0.005	Good	
			Vicon®	0.688±0.036	DGE: VI	0.872	0.001	Good	
Stride time (s)	L		DGE	1.166±0.127			\		
			Zebris®	1.152±0.126	DGE: ZE	0.936	0.000	Excellent	
			Vicon®	1.126±0.107	DGE: VI	0.832	0.000	Good	
	R		DGE	1.174±0.118				\	
			Zebris®	1.138±0.118	DGE: ZE	0.933	0.000	Excellent	
			Vicon®	1.139±0.127	DGE: VI	0.893	0.000	Good	
stance time	L		DGE	0.693±0.051			\		
			Zebris®	0.689±0.087	DGE: ZE	0.774	0.013	Good	
			Vicon®	0.696±0.035	DGE: VI	0.893	0.000	Good	
	R		DGE	0.687±0.102				\	
			Zebris®	0.694±0.056	DGE: ZE	0.711	0.026	General	
			Vicon®	0.691±0.124	DGE: VI	0.765	0.005	Good	
swing time	L		DGE	0.442±0.081			\		
			Zebris®	0.426±0.054	DGE: ZE	0.655	0.102	General	
			Vicon®	0.434±0.074	DGE: VI	0.895	0.000	Good	
	R		DGE	0.435±0.048				\	
			Zebris®	0.428±0.027	DGE: ZE	0.783	0.034	Good	
			Vicon®	0.439±0.039	DGE: VI	0.819	0.028	Good	
Cadence (Steps/min)	\		DGE	103.200±11.371			\		
			Zebris®	105.700±11.681	DGE: ZE	0.941	0.000	Excellent	
			Vicon®	106.860±11.601	DGE: VE	0.898	0.000	Good	
Step speed (m/s)	\		DGE	1.150±0.111			\		
			Zebris®	1.195±0.116	DGE: ZE	0.913	0.000	Excellent	
			Vicon®	1.217±0.114	DGE: VI	0.861	0.000	Good	
Stance phase (%)	L		DGE	61.400±2.366			\		
			Zebris®	62.940±1.610	DGE: ZE	0.574	0.110	General	
			Vicon®	61.820±1.120	DGE: VI	0.823	0.001	Good	
	R		DGE	61.600±2.319				\	
			Zebris®	63.640±2.465	DGE: ZE	0.724	0.034	General	
			Vicon®	62.031±1.872	DGE: VI	0.715	0.011	General	
Swing phase (%)	L		DGE	38.600±2.366			\		
			Zebris®	37.020±1.598	DGE: ZE	0.572	0.111	General	
			Vicon®	38.911±2.125	DGE: VI	0.682	0.000	General	
	R		DGE	38.500±2.369				\	
			Zebris®	36.360±2.465	DGE: ZE	0.720	0.036	General	
			Vicon®	37.241±2.157	DGE: VI	0.784	0.001	Good	
HS (°)	L		DGE	45.451±4.272			\		
			Vicon®	44.254±2.865	DGE: VI	0.521	0.202	General	

TABLE 3. (Continued.) DGE and Zebris®, Vicon® Intra-class correlation coefficient (ICC) and significance value of data statistics.

TO (°)	R	DGE	44.102±8.785	\		
		Vicon®	46.156±5.049	DGE: VI	0.587	0.108
	L	DGE	34.652±5.064	\		
		Vicon®	35.354±3.448	DGE: VI	0.611	0.265
	R	DGE	35.362±4.582	\		
		Vicon®	34.489±6.312	DGE: VI	0.645	0.322

The results of the DGE and VI left foot data are as follows: step length results ($ICC=0.802$, $p = 0.012$) have good reliability, stride time results ($ICC=0.832$, $p = 0.000$) have good reliability, stance time results ($ICC=0.893$, $p = 0.000$) have good reliability, swing time results ($ICC=0.895$, $p = 0.000$) have good reliability, stance phase results ($ICC=0.823$, $p = 0.001$) have good reliability, swing phase results ($ICC=0.682$, $p = 0.000$) have general reliability, HS results ($ICC=0.521$, $p = 0.202$) have general reliability, and TO results ($ICC=0.611$, $p = 0.265$) have general reliability. The right foot data results are as follows: step length results ($ICC=0.872$, $p = 0.001$) have good reliability, stride time results ($ICC=0.893$, $p = 0.000$) have good reliability, stance time results ($ICC=0.765$, $p = 0.005$) have good reliability, swing time results ($ICC=0.819$, $p = 0.028$) have good reliability, stance phase results ($ICC=0.715$, $p = 0.011$) have general reliability, swing phase results ($ICC=0.784$, $p = 0.001$) have good reliability, HS results ($ICC=0.587$, $p = 0.108$) have general reliability, and TO results ($ICC=0.645$, $p = 0.322$) have general reliability. Where the results of the cadence data are as follows: The reliability of DGE with ZE results ($ICC=0.969$, $p = 0.000$) is excellent and DGE with VI results ($ICC=0.946$, $p = 0.000$) is excellent. The results of the step data are as follows: DGE with ZE results ($ICC=0.913$, $p = 0.000$) have excellent reliability, and DGE with VI results ($ICC=0.861$, $p = 0.000$) have good reliability.

It is clear from Table 4 that for step length, stride time, cadence, HS, TO, and step speed in the DGE-ZE and DGE-VI groups, the difference between the means is not statistically significant and there is no significant difference (both p is greater than 0.05); for stance phase and swing phase in the DGE-ZE group are statistically significant and there is a significant difference (both p is less than 0.05 and greater than 0.01).

C. GROUP B: DIFFERENCES IN GAIT CHARACTERISTICS BETWEEN EPD PATIENTS AND HEALTHY INDIVIDUALS

For EPD patients and HT subjects were calculated: stride length, stride speed, cadence, stride time, stance time, swing time, HS angle, TO angle, stance phase and swing phase, and the results were calculated using the mean and standard deviation of each of the 6 steps for all test subjects. The results are shown in Table 5.

As shown (a) in Fig. 7, where EPD patients had significantly shorter stride lengths, slower stride speeds, reduced cadence, and overall longer stride time compared to HT subjects. From Table 5 It can be seen that the stance time to stride cycle ratio (64.25%) and swing time to stride cycle ratio (35.75%) in EPD patients and stance time to stride cycle ratio (62.42%) and swing time to stride cycle ratio (37.58%) in HT subjects; it can be seen that the stance time to stride cycle ratio increased in EPD patients and swing time to stride cycle ratio decreased in HT subjects compared to HT subjects. The difference between the toe-off angle of HT and EPD is small and the heel-off angle is large, and the heel-off angle may become a new parameter to distinguish HT from EPD.

The gait variability coefficients are recorded in Table 6. As shown (b) in Fig. 7, it can be seen that EPD patients had higher stride variability, stride time variability, swing phase variability and stance phase variability than HT subjects. Among them, the stride time variability and swing phase variability of EPD patients differed more than those of HT subjects.

D. GROUP B: EPD PATIENT ASSESSMENT RESULTS

Use a DT classifier to classify EPD patients and healthy participants, select 14 features using RFE, and select the optimal feature combination. We selected the feature combinations with the first to eighth importance scores from the RFE results (Fig. 8) and performed DT training sequentially, and found that the best classification combinations were those with the top six importance scores, i.e., the top six combinations achieved the best results in DT training. Therefore, the selected feature combinations are stride length, stance phase, stance time, swing phase variability, step speed and cadence. DT-RFE had a mean accuracy of 91.6%, specificity of 83%, sensitivity of 91% and ROC value of 0.92 for the classification of patients with EPD. In conclusion, the DGE system was shown to be effective in identifying patients with EPD.

VI. DISCUSSION

With the development of the gait field, gait problems have been taken seriously by scientific researchers in many fields. From the gait problem, the walking style of a person can be analyzed, and identification can be realized, etc. From the comparison of the gait of a class of people with certain

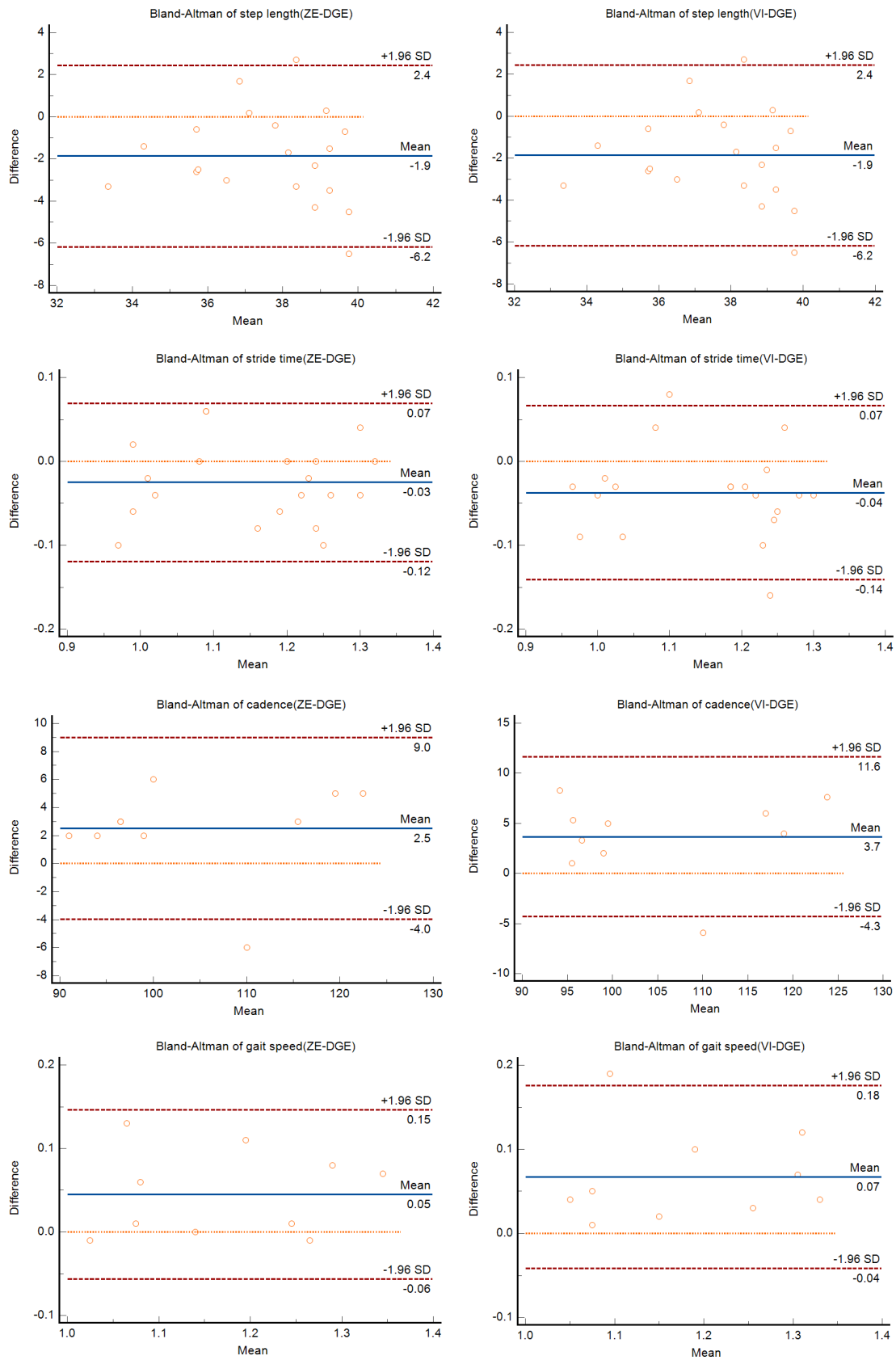


FIGURE 6. Differences between DGE and ZE and VI represented by Bland-Altman plots.

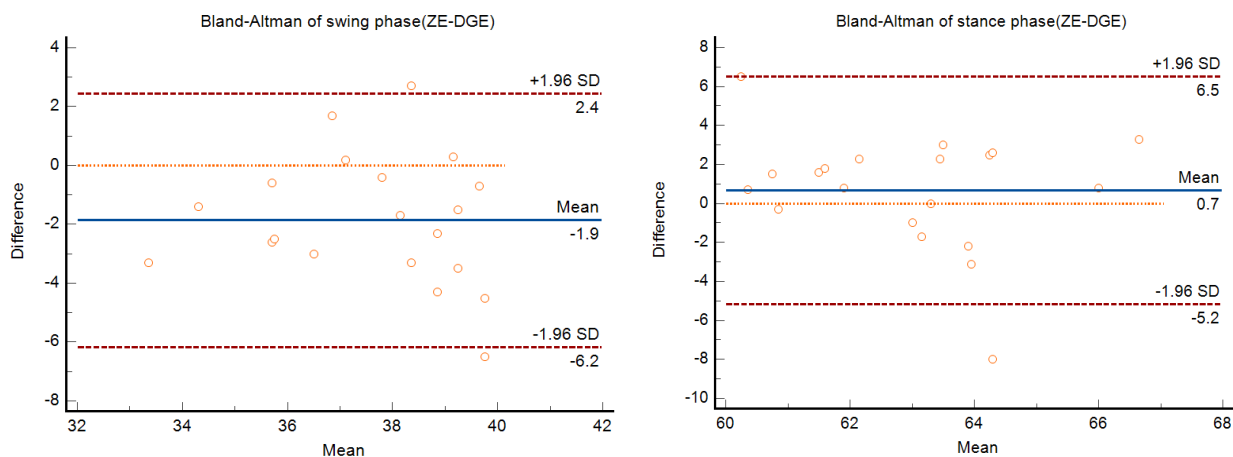


FIGURE 6. (Continued.) Differences between DGE and ZE and VI represented by Bland-Altman plots.

TABLE 4. DGE t-test with spatiotemporal parameters of ZE and VI systems, respectively.

	t-test comparison group	p
Step length	DGE-ZE	0.501
	DGE-VI	0.242
Stride time	DGE-ZE	0.511
	DGE-VI	0.316
Stance time	DGE-ZE	0.411
	DGE-VI	0.463
Swing time	DGE-ZE	0.362
	DGE-VI	0.244
Cadence	DGE-ZE	0.634
	DGE-VI	0.485
Step speed	DGE-ZE	0.388
	DGE-VI	0.201
Stance phase	DGE-ZE	0.013
	DGE-VI	0.422
Swing phase	DGE-ZE	0.010
	DGE-VI	0.264
HS	DGE-VI	0.365
TO	DGE-VI	0.624

characteristics with the normal healthy gait, the classification of people with this class of characteristics can be realized, etc. Long-term research has now demonstrated that gait is not limited to clinical and specific medical studies but also provides important indicators in the areas of post-operative rehabilitation, training, sports, and growing adolescents [37]. The feedback through gait has an important impact on the maintenance of health issues. With the multi-disciplinary

TABLE 5. HT and PD spatiotemporal gait parameters.

	HT(mean and SD)	EPD(mean and SD)
Stride length	1.21±0.09	0.97±0.12
Step speed	1.13±0.12	0.85±0.14
Cadence	111.83±5.20	104.38±9.07
Stride time	1.08±0.05	1.16±0.11
Stance time	0.67±0.05	0.75±0.09
Swing time	0.40±0.01	0.41±0.02
HS (°)	45.86±4.12	43.00±6.75
TO (°)	34.89±1.45	28.89±5.72
Stance phase	62.42±1.40	64.25±2.28
Swing phase	37.58±1.40	35.75±2.28

focus on gaits, relying solely on optical capture by cameras or fixed pressure plate runways is no longer sufficient, and secondly, they are very expensive, the former for light and the difference due to markers will also have reliability problems exist, the latter will be limited by the length of the path there are limitations of the activity. With the development of IMU being used as a gait field, it has some advantages such as being portable, cheap, wearable, and easy to maintain, most researchers have turned their attention to IMU research. For the development of IMU, the question of its accuracy and whether it can be used to replace expensive inspection equipment still needs to be continuously verified.

We first developed the DGE, proposing an IMU-based model capable of detecting daily gait. With low-power Bluetooth to view important parameters such as gait data, COP curve and ankle angle in real-time at the user's end. We performed the first parametric validation with the double gold standard to verify the validity of its data.

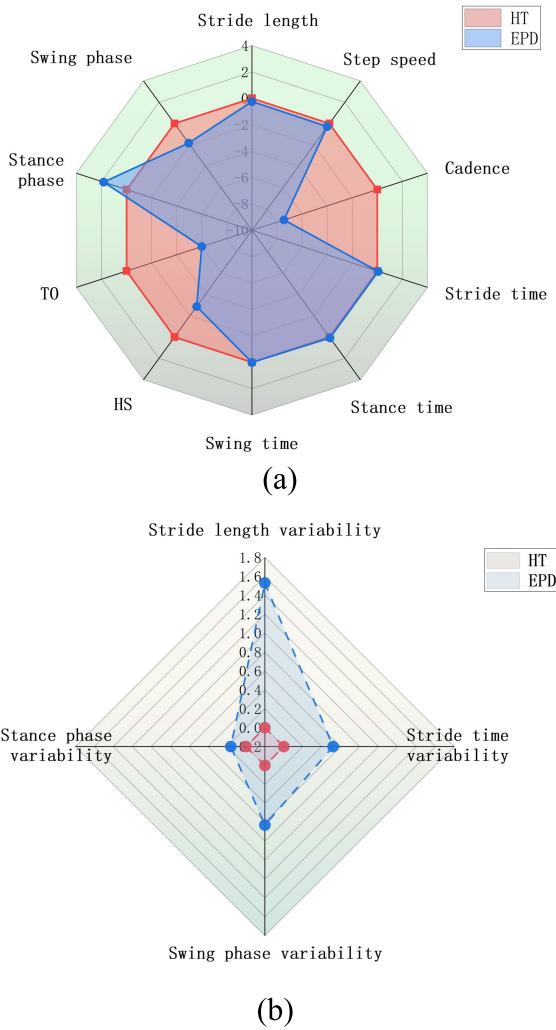


FIGURE 7. (a) ; Difference between HT and PD space-time gait parameters, (b); Difference between HT and PD gait variation coefficients.

TABLE 6. HT and PD gait variability.

	HT	EPD
Stride length variability (%)	5.11±1.99	6.64±4.31
Stride time variability (%)	1.74±0.98	2.26±0.98
Swing phase variability (%)	2.66±1.01	3.29±0.30
Stance phase variability (%)	1.60±0.62	1.76±0.24

A. DOUBLE GOLD STANDARD VERIFICATION

According to our survey, we found that there are few validation experiments for the new inertial sensor wearable gait detection devices, and most of them are still in the R&D stage or have a large gap with the gold standard that currently exists. Only a small number of spatiotemporal gait experiments have been validated in the current validation studies [38], [39], mostly using a single gold standard [40], [41], and most of the validation-type articles use Zebris® and Vicon® as gold standards. Thus, we used the double gold standard for

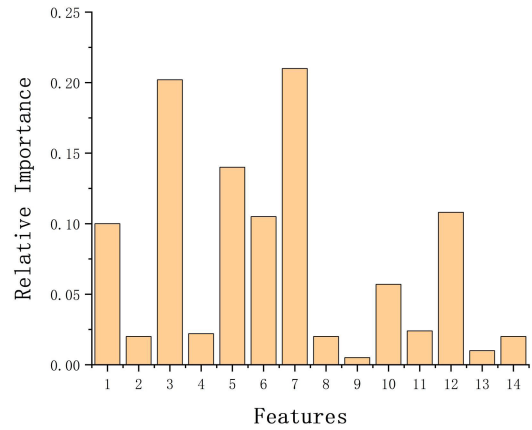


FIGURE 8. REF feature selection results. 1; Cadence, 2; HS, 3; Stance phase, 4; Stance phase variability, 5; Stance time, 6; Step speed, 7; Stride length, 8; Stride length variability, 9; Stride time, 10; Stride time variability, 11; Swing phase, 12; Swing phase variability, 13; Swing time, 14; TO.

the first time under the premise of using the single gold standard. Using the double gold standard can verify the consistency between this system and the current commonly used gold standard, and the results show that: DGE-Zebris has good overall reliability ($ICC \geq 0.572$) and DGE-Vicon has good overall reliability ($ICC \geq 0.521$). For most of the measured temporal gait parameters, the differences were within ± 1.96 SD with good agreement. It provides a good guarantee of data accuracy for the subsequent use of inertial sensors for wearable detection of gait in life and provides the necessary basic experimental validation for data sharing.

B. TEMPORAL GAIT AND VARIABILITY IN EPD PATIENTS

In this study, we collected only 30 patients with EPD (H&Y stage 1 and 2), and patients with intermediate and late stages were not included in this study, to verify the detectability of DGE in EPD patients on the one hand, and to distinguish EPD patients from healthy gait patients of the same age on the other hand, which has a distinguishable meaning. In the study of gait in EPD patients, Jakob et al. were unable to identify different gait parameters between EPD and healthy controls in straight-line walking [42], and Yang et al. proposed an IMU model to detect EPD patients during turns, but it is still difficult to detect subtle differences in the gait in EPD patients in straight-line walking [16].

C. IMU ACCURACY ISSUES

For the IMU for measurement, there will be accuracy problems, the gyroscope has good dynamic response characteristics, but there will be integral cumulative error and the error caused by temperature drift; the accelerometer is good static stability, for dynamic calculation of the angle error is larger, so we need to correct the gyroscope through the accelerometer. To reduce the error accumulation problem caused by integration we need to reinitialize each new step

in the calculation, Hamacher et al. to verify that this method works [43].

The system was first validated against the gold standard to prove the reliability of its data, indicating that the data measured by DGE is universal. The prediction accuracy by DT-REF is 91.6% and the ROC value is 0.92, which proves that the model can predict early PD patients better, and the system is portable, convenient and can be used anytime and anywhere to do the test, which will reduce the expenditure of the pharmaceutical system.

D. WALKING COP CURVE PROVIDES BALANCE MEASURE FOR EPD PATIENTS

For the current stage of research, we first developed a foot wearable system that can be used to obtain real-time gait parameters in daily life, and can dynamically display foot pressure changes during walking in the form of a visualization chart, and draw the COP trajectory in walking, which can be used to measure the stability of daily walking, where the closer the COP walking trajectory is to a straight line the better the balance of the tester's walking.

E. CLINICAL SIGNIFICANCE AND ROLE OF THE RESULTS

Although it is generally accepted in current research that resting tremor, bradykinesia and rigidity are the main symptoms of PD [44]. But abnormal movements, as well as small changes in posture, may be evident from the early stages of Parkinson's, where reduced gait length is one of the key features of gait, a finding that has been verified in previous studies [45]. The results of our experiments show that in addition to significant changes in stride length, there are also significant changes in the five parameters of stance phase, stance time, swing phase variability, step speed and cadence in patients with EPD. This may be a new confirmation that changes in these five parameters may provide the necessary test for the subsequent early detection of patients with EPD. The study of gait in EPD is still little studied by anyone. Some subtle changes in walking impairment may already be present in people with EPD. Through this experiment, it was demonstrated that a highly accurate differentiation between elderly EPD and healthy elderly individuals is feasible, or in the future, may provide a basis for medical testing and rehabilitation of EPD to prevent further deterioration of pathological movements and postures caused by long-term abnormal gait patterns.

In conclusion, this system allows for the study of EPD gait, which may provide a theoretical basis for future detection of EPD or physiotherapy strategies, and evidence that more accurate detection can be applied in clinical practice and may improve treatment outcomes.

F. LIMITATIONS

The number of samples collected in this experiment is small, and a large amount of data collection work has not been performed, and further validation is needed for a large number

of data results. The system designs to foot pressure and ankle joint angle is not validated for the time being and requires subsequent validation. In this study, we first validated the data of this system with the double gold standard, and secondly, we collected and compared the spatiotemporal gait data of early Parkinson's elderly patients with healthy elderly people, but these studies were cross-sectional and did not conduct longitudinal studies. Due to equipment limitations, we did not validate the gait data in daily life.

VII. CONCLUSION

Through effective experimental comparison with Zebris® and Vicon® double gold standards, DGE can provide effective measurement with accurate capture in step length, stride time, cadence, step speed, stance phase and swing phase gait parameters. And for the recruited EPD patients and recruited HT subjects, using DGE for measurement, we could get a significant difference between the gait parameters of EPD patients and HT subjects, which proved that the IMU-based detection system was able to detect subtle gait characteristics in straight-line walking, which provided a basis for our team to conduct the next study on the gait of Parkinson's patients. This system may in the future become an inexpensive alternative to expensive laboratory gait detection equipment and can be used in everyday life, in variable environments, and with high accuracy. In the future, we will recruit more patients with EPD as well as other patients who may develop gait disorders such as Alzheimer's patients as well for more in-depth studies. Whether certain parameters change in gait in patients with other early neurological disorders remains to be tested in our later experiments. DGE has higher accuracy and provides a good basis for our upcoming longitudinal study of gait in EPD patients, which can track gait changes in EPD patients and effectively reduce the inconvenience of longitudinal studies of EPD patients and save medical costs.

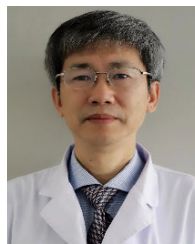
REFERENCES

- [1] C. G. Canning, S. S. Paul, and A. Nieuwboer, "Prevention of falls in Parkinson's disease: A review of fall risk factors and the role of physical interventions," *Neurodegenerative Disease Manage.*, vol. 4, no. 3, pp. 203–221, Jun. 2014, doi: [10.2217/nmt.14.22](https://doi.org/10.2217/nmt.14.22).
- [2] E. Berra, R. D. Icco, M. Avenali, C. Dagna, S. Cristina, C. Pacchetti, M. Fresia, G. Sandrini, and C. Tassorelli, "Body weight support combined with treadmill in the rehabilitation of parkinsonian gait: A review of literature and new data from a controlled study," *Frontiers Neurol.*, vol. 9, p. 1066, Feb. 2019, doi: [10.3389/fneur.2018.01066](https://doi.org/10.3389/fneur.2018.01066).
- [3] T. Ellis, J. T. Cavanaugh, G. M. Earhart, M. P. Ford, K. B. Foreman, and L. E. Dibble, "Which measures of physical function and motor impairment best predict quality of life in Parkinson's disease?" *Parkinsonism Rel. Disorders*, vol. 17, no. 9, pp. 693–697, Nov. 2011, doi: [10.1016/j.parkreldis.2011.07.004](https://doi.org/10.1016/j.parkreldis.2011.07.004).
- [4] B. Galna, S. Lord, D. J. Burn, and L. Rochester, "Progression of gait dysfunction in incident Parkinson's disease: Impact of medication and phenotype," *Movement Disorders*, vol. 30, no. 3, pp. 359–367, Mar. 2015, doi: [10.1002/mds.26110](https://doi.org/10.1002/mds.26110).
- [5] M. Hoehn and M. Yahr, "Parkinsonism: Onset, progression, and mortality," *Neurology*, vol. 77, no. 9, p. 874, Aug. 2011.
- [6] M. E. Morris, "Movement disorders in people with Parkinson disease: A model for physical therapy," *Phys. Therapy*, vol. 80, no. 6, pp. 578–597, Jun. 2000, doi: [10.1093/ptj/80.6.578](https://doi.org/10.1093/ptj/80.6.578).

- [7] S. Oveisgharan, L. Yu, D. A. Bennett, and A. S. Buchman, "Incident mobility disability, parkinsonism, and mortality in community-dwelling older adults," *PLoS One*, vol. 16, no. 2, Feb. 2021, Art. no. e0246206, doi: [10.1371/journal.pone.0246206](https://doi.org/10.1371/journal.pone.0246206).
- [8] C. G. Goetz et al., "Movement disorder society-sponsored revision of the unified Parkinson's disease rating scale (MDS-UPDRS): Scale presentation and clinimetric testing results," *Movement Disorders*, vol. 23, no. 15, pp. 2129–2170, Nov. 2008, doi: [10.1002/mds.22340](https://doi.org/10.1002/mds.22340).
- [9] M. Pau, F. Corona, R. Pili, C. Casula, M. Guicciardi, G. Cossu, and M. Murgia, "Quantitative assessment of gait parameters in people with Parkinson's disease in laboratory and clinical setting: Are the measures interchangeable?" *Neurol. Int.*, vol. 10, no. 2, p. 7729, Jul. 2018.
- [10] A. Mirelman, L. Rochester, I. Maidan, S. D. Din, L. Alcock, F. Nieuwhof, M. O. Rikkert, B. R. Bloem, E. Pelosin, L. Avanzino, G. Abbruzzese, K. Dockx, E. Bekkers, N. Giladi, A. Nieuwboer, and J. M. Hausdorff, "Addition of a non-immersive virtual reality component to treadmill training to reduce fall risk in older adults (V-TIME): A randomised controlled trial," *Lancet*, vol. 388, no. 10050, pp. 1170–1182, 2016, doi: [10.1016/S0140-6736\(16\)31325-3](https://doi.org/10.1016/S0140-6736(16)31325-3).
- [11] A. Mirelman, P. Bonato, R. Camicioli, T. D. Ellis, N. Giladi, J. L. Hamilton, C. J. Hass, J. M. Hausdorff, E. Pelosin, and Q. J. Almeida, "Gait impairments in Parkinson's disease," *Lancet Neurol.*, vol. 18, no. 9, pp. 697–708, 2019, doi: [10.1016/S1474-4422\(19\)30044-4](https://doi.org/10.1016/S1474-4422(19)30044-4).
- [12] J. L. Lanovaz, A. R. Oates, T. T. Treen, J. Unger, and K. E. Musselman, "Validation of a commercial inertial sensor system for spatiotemporal gait measurements in children," *Gait Posture*, vol. 51, pp. 14–19, Jan. 2017, doi: [10.1016/j.gaitpost.2016.09.021](https://doi.org/10.1016/j.gaitpost.2016.09.021).
- [13] C. L. Pulliam, D. A. Heldman, E. B. Brokaw, T. O. Mera, Z. K. Mari, and M. A. Burack, "Continuous assessment of levodopa response in Parkinson's disease using wearable motion sensors," *IEEE Trans. Biomed. Eng.*, vol. 65, no. 1, pp. 159–164, Jan. 2018, doi: [10.1109/TBME.2017.2697764](https://doi.org/10.1109/TBME.2017.2697764).
- [14] B. Najafi, T. Khan, and J. Wrobel, "Laboratory in a box: Wearable sensors and its advantages for gait analysis," in *Proc. Annu. Int. Conf. IEEE Eng. Med. Biol. Soc.*, Apr. 2011, pp. 6507–6510.
- [15] C. Curtze, J. G. Nutt, P. Carlson-Kuhta, M. Mancini, and F. B. Horak, "Levodopa is a double-edged sword for balance and gait in people with Parkinson's disease," *Movement Disorders*, vol. 30, no. 10, pp. 1361–1370, Sep. 2015, doi: [10.1002/mds.26269](https://doi.org/10.1002/mds.26269).
- [16] Y. Yang, L. Chen, J. Pang, X. Huang, L. Meng, and D. Ming, "Validation of a spatiotemporal gait model using inertial measurement units for early-stage Parkinson's disease detection during turns," *IEEE Trans. Biomed. Eng.*, vol. 69, no. 12, pp. 3591–3600, Dec. 2022, doi: [10.1109/TBME.2022.3172725](https://doi.org/10.1109/TBME.2022.3172725).
- [17] X. Wu, Y. Wang, and G. Pottie, "A robust step length estimation system for human gait using motion sensors," in *Proc. Conf. Wireless Health*, Oct. 2015, pp. 1–5.
- [18] L. Pepa, G. Marangoni, M. Di Nicola, L. Ciabattini, F. Verdini, L. Spalazzi, and S. Longhi, "Real time step length estimation on smartphone," in *Proc. IEEE Int. Conf. Consum. Electron. (ICCE)*, Jan. 2016, pp. 315–316.
- [19] L. Wang, Y. Sun, Q. Li, and T. Liu, "Estimation of step length and gait asymmetry using wearable inertial sensors," *IEEE Sensors J.*, vol. 18, no. 9, pp. 3844–3851, May 2018, doi: [10.1109/JSEN.2018.2815700](https://doi.org/10.1109/JSEN.2018.2815700).
- [20] B. Anderson, M. Shi, V. Y. F. Tan, and Y. Wang, "Mobile gait analysis using foot-mounted UWB sensors," in *Proc. ACM Interact., Mobile, Wearable Ubiquitous Technol.*, Sep. 2019, vol. 3, no. 3, pp. 1–22, doi: [10.1145/3351231](https://doi.org/10.1145/3351231).
- [21] F. Lin, A. Wang, Y. Zhuang, M. R. Tomita, and W. Xu, "Smart insole: A wearable sensor device for nonobtrusive gait monitoring in daily life," *IEEE Trans. Ind. Informat.*, vol. 12, no. 6, pp. 2281–2291, Dec. 2016, doi: [10.1109/TII.2016.2585643](https://doi.org/10.1109/TII.2016.2585643).
- [22] Y. Yang, "Spacecraft attitude determination and control: Quaternion based method," *Annu. Rev. Control*, vol. 36, no. 2, pp. 198–219, Dec. 2012, doi: [10.1016/j.arcontrol.2012.09.003](https://doi.org/10.1016/j.arcontrol.2012.09.003).
- [23] V. Kubelka and M. Reinstein, "Complementary filtering approach to orientation estimation using inertial sensors only," in *Proc. IEEE Int. Conf. Robot. Autom.*, May 2012, pp. 599–605.
- [24] T. Hiller, Z. Pentek, J.-T. Liewald, A. Buhmann, and H. Roth, "Origins and mechanisms of bias instability noise in a three-axis mode-matched MEMS gyroscope," *J. Microelectromech. Syst.*, vol. 28, no. 4, pp. 586–596, Aug. 2019, doi: [10.1109/JMEMS.2019.2921607](https://doi.org/10.1109/JMEMS.2019.2921607).
- [25] M. M. Konor, S. Morton, J. M. Eckerson, and T. L. Grindstaff, "Reliability of three measures of ankle dorsiflexion range of motion," *Int. J. Sports Phys. Therapy*, vol. 7, no. 3, 2012, pp. 87–279.
- [26] J. W. Kim, H. J. Jang, D.-H. Hwang, and C. Park, "A step, stride and heading determination for the pedestrian navigation system," *J. Global Positioning Syst.*, vol. 3, nos. 1–2, pp. 273–279, Dec. 2004, doi: [10.5081/jgps.3.1.273](https://doi.org/10.5081/jgps.3.1.273).
- [27] J. A. Mercer, J. Vance, A. Hreljac, and J. Hamill, "Relationship between shock attenuation and stride length during running at different velocities," *Eur. J. Appl. Physiol.*, vol. 87, nos. 4–5, pp. 8–403, Aug. 2002, doi: [10.1007/s00421-002-0646-9](https://doi.org/10.1007/s00421-002-0646-9).
- [28] J. Scarlett, "Enhancing the performance of pedometers using a single accelerometer," *Appl. Note, Analog Devices*, vol. 41, pp. 1–16, Mar. 2007.
- [29] P. Skorga and C. F. Young, "Mini-mental state examination for the detection of Alzheimer disease and other dementias in people with mild cognitive impairment," *Clin. Nurse Specialist*, vol. 29, no. 5, pp. 265–267, 2015.
- [30] C. G. Goetz, W. Poewe, O. Rascol, C. Sampaio, G. T. Stebbins, C. Counsell, N. Giladi, R. G. Holloway, C. G. Moore, G. K. Wenning, M. D. Yahr, and L. Seidl, "Movement Disorder society task force report on the Hoehn and Yahr staging scale: Status and recommendations The Movement Disorder society task force on rating scales for Parkinson's disease," *Movement Disorders*, vol. 19, no. 9, pp. 1020–1028, Sep. 2004, doi: [10.1002/mds.20213](https://doi.org/10.1002/mds.20213).
- [31] K. V. Alsenoy, A. Thomson, and A. Burnett, "Reliability and validity of the Zebris FDM-THQ instrumented treadmill during running trials," *Sports Biomech.*, vol. 18, no. 5, pp. 501–514, Sep. 2019, doi: [10.1080/14763141.2018.1452966](https://doi.org/10.1080/14763141.2018.1452966).
- [32] B. Westhoff, M. Hirsch, H. Hefter, A. Wild, and R. Krauspe, "How reliable are data from 3D-gait analysis," *Sportverletzung Sportschaden*, vol. 18, no. 2, pp. 76–79, 2004.
- [33] S. Kesikburun, "Effect of ankle foot orthosis on gait parameters and functional ambulation in patients with stroke," *Turkish J. Phys. Med. Rehabil.*, vol. 63, no. 2, pp. 143–148, Jun. 2017, doi: [10.5606/tftrd.2017.129](https://doi.org/10.5606/tftrd.2017.129).
- [34] R. Pullanagari, G. Kereszturi, and I. Yule, "Integrating airborne hyperspectral, topographic, and soil data for estimating pasture quality using recursive feature elimination with random forest regression," *Remote Sens.*, vol. 10, no. 7, p. 1117, Jul. 2018, doi: [10.3390/rs10071117](https://doi.org/10.3390/rs10071117).
- [35] A. Priyam, G. Abhijeeta, A. Rathee, and S. Srivastava, "Comparative analysis of decision tree classification algorithms," *Int. J. Current Eng. Technol.*, vol. 3, no. 2, pp. 334–337, 2013.
- [36] S. D. Jadhav and H. P. Channe, "Comparative study of K-NN, naive Bayes and decision tree classification techniques," *Int. J. Sci. Res.*, vol. 5, no. 1, pp. 1842–1845, 2016.
- [37] M. Akhtaruzzaman, A. A. Shafie, and R. Khan, "Gait analysis: Systems, technologies, and importance," *J. Mech. Med. Biol.*, vol. 16, no. 7, pp. 331–342, 2016, doi: [10.1142/S0219519416300039](https://doi.org/10.1142/S0219519416300039).
- [38] G. T. Burns, J. D. Zender, and R. F. Zernicke, "Validation of a wireless shoe insole for ground reaction force measurement," *J. Sports Sci.*, vol. 37, no. 2, pp. 1–10, 2018, doi: [10.1080/02640414.2018.1545515](https://doi.org/10.1080/02640414.2018.1545515).
- [39] B. J. Braun, N. T. Veith, R. Hell, S. Döbele, M. Roland, M. Rollmann, J. Holstein, and T. Pohlemann, "Validation and reliability testing of a new, fully integrated gait analysis insole," *J. Foot Ankle Res.*, vol. 8, no. 1, pp. 1–7, Dec. 2015, doi: [10.1186/s13047-015-0111-8](https://doi.org/10.1186/s13047-015-0111-8).
- [40] Y.-S. Cho, S.-H. Jang, J.-S. Cho, M.-J. Kim, H. D. Lee, S. Y. Lee, and S.-B. Moon, "Evaluation of validity and reliability of inertial measurement unit-based gait analysis systems," *Ann. Rehabil. Med.*, vol. 42, no. 6, pp. 872–883, Dec. 2018, doi: [10.5535/arm.2018.42.6.872](https://doi.org/10.5535/arm.2018.42.6.872).
- [41] E. Ziagkas, A. Loukovitis, D. X. Zekakos, T. D.-P. Chau, A. Petrelis, and G. Grouios, "A novel tool for gait analysis: Validation study of the smart insole PODOSmar[®]," *Sensors*, vol. 21, no. 17, p. 5972, Sep. 2021, doi: [10.3390/s21175972](https://doi.org/10.3390/s21175972).
- [42] V. Jakob, A. Küderle, F. Kluge, J. Klucken, B. M. Eskofier, J. Winkler, M. Winterholler, and H. Gassner, "Validation of a sensor-based gait analysis system with a gold-standard motion capture system in patients with Parkinson's disease," *Sensors*, vol. 21, no. 22, p. 7680, Nov. 2021, doi: [10.3390/s21227680](https://doi.org/10.3390/s21227680).
- [43] D. Hamacher, D. Hamacher, W. R. Taylor, N. B. Singh, and L. Schega, "Towards clinical application: Repetitive sensor position re-calibration for improved reliability of gait parameters," *Gait Posture*, vol. 39, no. 4, pp. 1146–1148, Apr. 2014.
- [44] S. Sveinbjornsdottir, "The clinical symptoms of Parkinson's disease," *J. Neurochem.*, vol. 139, pp. 318–324, Oct. 2016.
- [45] M. Pistacchi, "Gait analysis and clinical correlations in early Parkinson's disease," *Funct. Neurol.*, vol. 32, no. 1, p. 28, 2017.



SHUAI TAO received the degree in computer science from Hokkaido University, Japan, and the Ph.D. degree. He is currently a Professor with the School of Information Science, Dalian University, China. He is mainly engaged in the research and development of medical smart wearable devices, mobile internet and big data technology, and other related directions. He is dedicated to the research of gait big data and the whole course management of cognitive disorders in the elderly, intelligent diagnosis, disease course identification, efficacy assessment, and rehabilitation of cognitive disorders.



ZEPING LV received the master's degree in medicine. He is currently a Chief Neurologist. He is also a Chief Physician with the Department of Neurology. His main research interests are clinical neurology and neurorehabilitation. He specializes in the diagnosis and treatment of neurodegenerative diseases (mainly Alzheimer's disease and Parkinson's disease), especially those related to memory, cognition, and sleep, and the prevention, treatment, and rehabilitation of cerebrovascular diseases.



HAOYE WANG is currently pursuing the master's degree in control science and control engineering with Dalian University, China. His main research interests are wearable devices and intelligent diagnosis for patients with early Parkinson's disease.



LIWEN KONG is currently pursuing the Ph.D. degree with Tianjin University, China. She is currently a Lecturer with the School of Electronic Information Engineering, Dalian University, China. She is mainly engaged in the research and development of medical smart wearable devices, mobile internet and big data technology, and other related directions.



ZUMIN WANG received the Ph.D. degree. He is currently a Professor with the School of Information Science, Dalian University, China. He has presided over nearly 20 research projects of various kinds and published more than 50 academic articles. His main research interests are the IoT technology, smart medical, and smart agriculture.

...